

Irreversibility of the two-dimensional enstrophy cascade

E. Piretto¹, S. Musacchio² and G. Boffetta¹

¹*Department of Physics and INFN, Università di Torino, via P. Giuria 1, 10125 Torino, Italy*

²*Université de Nice Sophia Antipolis, CNRS, LJAD, UMR 7351, 06100 Nice, France*

(Dated: September 25, 2018)

We study the time irreversibility of the direct cascade in two-dimensional turbulence by looking at the time derivative of the square vorticity along Lagrangian trajectories, a quantity which we call *metenstrophy*. By means of extensive numerical simulations we measure the time irreversibility from the asymmetry of the PDF of the metenstrophy and we find that it increases with the Reynolds number of the cascade, similarly to what found in three-dimensional turbulence. A detailed analysis of the different contributions to the enstrophy budget reveals a remarkable difference with respect to what observed for the direct cascade, in particular the role of the statistics of the forcing to determine the degree of irreversibility.

I. INTRODUCTION

Although the time reversibility of the Navier-Stokes equations is broken by the viscous forces, it is not restored in the limit of vanishing viscosity. Indeed in this limit one obtains the regime of fully developed turbulence, characterized by an irreversible flux of energy from the large scales to the small scales where it is dissipated. The irreversibility of the energy flux in three-dimensional turbulence is responsible for the asymmetry of the *two-point* statistical observables, either in a fixed Eulerian reference frame as in the case of velocity structure functions which display a negative third moment [1], or for the Lagrangian evolution of pairs of trajectories [2].

Recently, it has been shown on the basis of laboratory experiments and numerical simulations, how irreversibility in turbulence manifests at the level of *single-point* observable [3]. By looking at the evolution of the energy along a fluid trajectory, it has been shown that the particle acquires (kinetic) energy on a long time scale and loses it on a short time scale. This reflects the fact that energy is injected in the flow by an external forcing at large, slow scales and is dissipated by viscosity at small, fast scales [4]. As a consequence, although in stationary conditions the mean temporal increment of energy vanishes, the full statistics is not time-reversible and odd moments of energy increments are different from zero [3]. Time irreversibility can be quantified by looking at the statistics of the power along a trajectory $p(t) = d/dt(v^2(t)/2)$ and it has been shown that the third moment $\langle p^3 \rangle$ is negative and increases with the control parameter, the Reynolds number, of the flow. Similar results have been found for the inverse cascade of energy in two-dimensional turbulence, which is characterized by the same scaling law of 3D turbulence [5] and in compressible turbulence [6]. Despite the fact that in 2D the energy flows towards the large scales (instead of the small scales), time irreversibility manifests in two-dimensional turbulence as in 3D, with a negative skewness of the power computed along a Lagrangian trajectory [3].

In this paper, we study the time irreversibility of the *direct cascade* in two-dimensional turbulence, characterized by an enstrophy (mean square vorticity) flow towards

small scales, by studying the statistics of what we call *metenstrophy*, i.e. the time derivative of the enstrophy along a trajectory. The main motivation for this work is that the direct cascade is characterized by a single characteristic time [5] and therefore spatial separation (between injection and dissipation scales) does not corresponds in a simple way to time-scale separation. This make this turbulence completely different from the energy cascades (direct and inverse) studied in [3]. On the basis of direct numerical simulations at different Reynolds number, we find that also in this case single-point statistics breaks time reversal symmetry and that the degree of irreversibility grows with the Reynolds numbers of the flow. A part this similarity, the picture which emerges from the direct enstrophy cascade is very different from what observed in the energy cascade, as here the terms that contributes to the enstrophy balance are all local and pressure gradient, which is responsible for the transfer of energy from slow to fast particles in 3D [7] is absent.

The remaining of this paper is organized as follow. In Section II we provide a brief survey of two-dimensional turbulence, introducing the equations and the main quantities which will be discussed in the paper. In Section III we report the results of our numerical simulations. Section IV is devoted to the discussion of our findings.

II. THEORETICAL BACKGROUND

We consider the two-dimensional, incompressible Navier-Stokes equation for the vorticity field $\omega = \partial_x u_y - \partial_y u_x$ in a double periodic square box of dimension $L \times L$

$$\partial_t \omega + \mathbf{u} \cdot \nabla \omega = \nu \nabla^2 \omega - \alpha \omega + f \quad (1)$$

where ν is the kinematic viscosity, α the friction coefficient and $f(\mathbf{x}, t)$ is an external forcing needed to sustain a stationary state. In the inviscid ($\nu = \alpha = 0$) unforced ($f = 0$) limit (1) has two conserved quantities: kinetic energy $E = (1/2)\langle u^2 \rangle$ and enstrophy $Z = (1/2)\langle \omega^2 \rangle$. Here $\langle \dots \rangle$ represent average over the L^2 domain). The forcing term f inject energy and enstrophy at a characteristic

scale in the system from which energy and enstrophy are transported towards large and small scales respectively, generating the double cascade predicted by Kraichnan 50 years ago [5, 8]. The inverse cascade of energy is characterized by Kolmogorov-like spectrum with close-to-Gaussian statistics [9] and its time-reversal properties have been object of previous works [3, 7]. In the direct cascade to small scales, enstrophy is transferred at a rate η from the forcing scales ℓ_f down to the dissipative scales $\ell_\nu \sim \nu^{1/2}/\eta^{1/6}$ generating a power spectrum with exponent close to the dimensional prediction -3 [10–17]. The ratio of these scales defines the Reynolds number of the cascade as $Re = \eta^{1/3}\ell_f^2/\nu = (\ell_f/\ell_\nu)^2$.

In presence of forcing and dissipation, the time derivative of the local square vorticity along a trajectory, which will be called *metenstrophy* q , is given by

$$q \equiv \frac{D}{Dt} \frac{1}{2} \omega^2 = q_\nu + q_\alpha + q_f \quad (2)$$

where with obvious notation we have introduced $q_\nu = \omega\nu\nabla^2\omega$, $q_\alpha = -\alpha\omega^2$ and $q_f = \omega f$. In stationary conditions we have $\langle q \rangle = 0$ and the enstrophy balance reads $\langle q_f \rangle = -\langle q_\nu \rangle - \langle q_\alpha \rangle$ where the viscous dissipation is equal to the enstrophy flux $-\langle q_\nu \rangle = \eta$, while the large scale enstrophy dissipation $\langle q_\alpha \rangle$ is negligible for large Reynolds numbers [9].

We observe that in the decomposition (2) all terms are local, involving products of the vorticity field and its derivatives. This is the main difference with respect to the balance for the energy cascade in which a non-local term given by the pressure gradient is present. Although the pressure forces on average do not contribute to the kinetic energy balance, in 3D they are responsible for the redistribution of energy from slow to fast particles and for the asymmetry of the PDF of energy power. The absence of the analogous of the pressure forces in (2) suggests that the statistics of metenstrophy in the 2D direct cascade will be very different from the statistics of power in 3D.

III. NUMERICAL RESULTS

We have integrated the Navier-Stokes Equations (1) on a doubly periodic square domain of size $L = 2\pi$ at resolution $N^2 = 1024^2$, by means of a standard fully-dealiased pseudospectral code, with 4th-order Runge-Kutta scheme with implicit integration of the linear dissipative terms. In order to avoid contamination of the enstrophy cascade [18] the linear friction term $-\alpha\omega$ has been replaced by an ipo-friction term $-\alpha\nabla^{-4}\omega$ which confines the dissipation to the largest scales.

Considering that the variations of the enstrophy along a Lagrangian trajectory are due only to the contributions of the forcing and dissipation, we have performed two sets of simulations aimed to investigate separately the effects of the viscous dissipation and of the external force on the metenstrophy statistics.

In the following, all the results are non-dimensionalized with the enstrophy flux η and with the characteristic time of the flow defined as $\tau_\omega = \eta^{-1/3}$.

A. Dependence on Reynolds

We performed a first set of simulation (Set A) to investigate the dependence of the statistics on the Reynolds number by gradually reducing the viscosity and keeping fixed the forcing. In these simulations we use a deterministic, time-independent force $f(x, y) = F \sin(k_f x) \sin(k_f y)$. The forcing scale is defined as $\ell_f = 2\pi/(k_f\sqrt{2})$ and the parameters of the simulations are reported in Table III A. The statistics is computed over 2000 independent vorticity fields, sampled every $1.2\tau_\omega$.

In Figure 1 we show the probability distribution functions (PDFs) of the metenstrophy q for the simulations of the Set A at different Reynolds numbers. Even if the mean value of q vanishes, because of the statistical time-stationarity, the full statistics reveals a noticeable violation of the time symmetry. In particular, at increasing Re we observe the development of a large left tail in the PDFs and the third moment of q become negative.

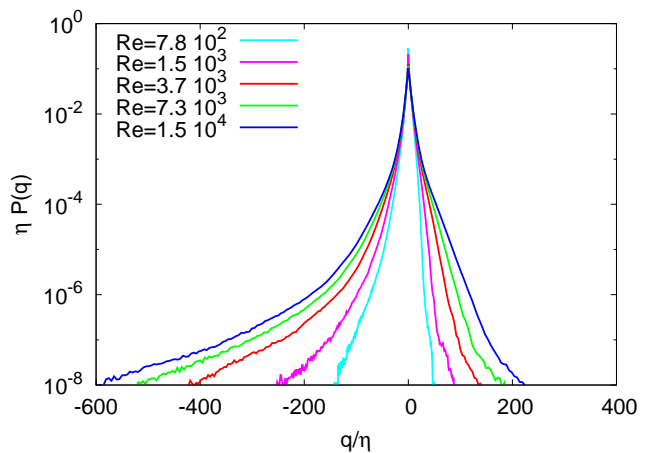


FIG. 1. (Color online). PDFs of metenstrophy q at increasing Re (from the inner to the outer PDF)

Both the second moment $\langle q^2 \rangle$ and the third moment $\langle q^3 \rangle$ of the distribution grow monotonically with Re (see Figure 2), similarly to what observed for the statistics of power in 3D turbulence [3]. At variance with the 3D case, here we are unable to find a clear power-law scaling for the two moments but this could still be due to finite Reynolds effect.

The skewness $S = \langle q^3 \rangle / \langle q^2 \rangle^{3/2}$ provides a suitable measure of the irreversibility. The results of our numerics show that it increases with Re (see Figure 2) and suggest a possible saturation to a constant value for large values of Re . We remark that the saturation of the skewness to a constant value has been observed for the power in 3D turbulence.

Re	ν	$-\langle q_\nu \rangle$	$-\langle q_\alpha \rangle$	$\langle q_f \rangle$	E	Z
$7.8 \cdot 10^2$	10^{-3}	$2.48 \cdot 10^{-1}$	$2.4 \cdot 10^{-2}$	$2.72 \cdot 10^{-1}$	$1.06 \cdot 10^{-1}$	1.99
$1.5 \cdot 10^3$	$5 \cdot 10^{-4}$	$2.24 \cdot 10^{-1}$	$2.8 \cdot 10^{-2}$	$2.53 \cdot 10^{-1}$	$1.30 \cdot 10^{-1}$	2.53
$3.7 \cdot 10^3$	$2 \cdot 10^{-4}$	$2.13 \cdot 10^{-1}$	$3.4 \cdot 10^{-2}$	$2.47 \cdot 10^{-1}$	$1.68 \cdot 10^{-1}$	3.62
$7.3 \cdot 10^3$	$1 \cdot 10^{-4}$	$2.07 \cdot 10^{-1}$	$3.7 \cdot 10^{-2}$	$2.44 \cdot 10^{-1}$	$1.38 \cdot 10^{-1}$	4.25
$1.5 \cdot 10^4$	$5 \cdot 10^{-5}$	$2.05 \cdot 10^{-1}$	$4.0 \cdot 10^{-2}$	$2.46 \cdot 10^{-1}$	$2.27 \cdot 10^{-1}$	5.75

TABLE I. Parameters of the simulations with deterministic forcing (Set A). The amplitude of the force is $F = 1$ and the forcing wavenumber $k_f = 4$. The ipo-friction coefficient is $\alpha = 1$.

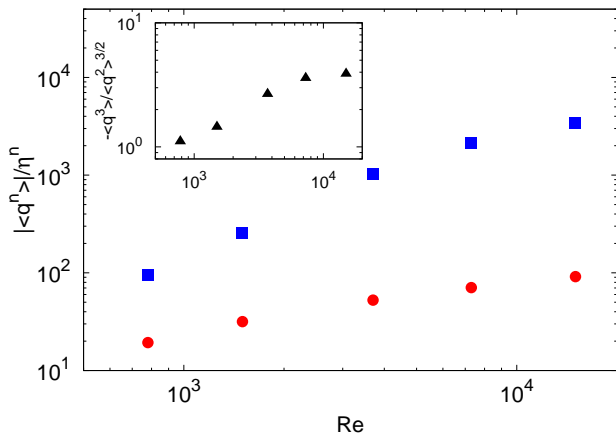


FIG. 2. (Color online). Second (red circles) and third (blue square) moments of the PDFs of metenstrophy q as a function of Re . Inset: Skewness of metenstrophy as a function of Re .

In order to understand which physical process is responsible for the breaking of the time-symmetry, we have analyzed the different contributions to the metenstrophy, due to the forcing q_f , the viscous dissipation q_ν and the ipo-friction q_α . In Figure 3 we compare the PDF of q for the run at $Re = 1.5 \cdot 10^4$ with the PDFs of q_f , q_ν and q_α . We find that the large left tail of the PDF of q , is dominated by local events of intense viscous dissipation, which can be 600 times more intense than their mean. Conversely, the statistics of the forcing contributions q_f is more symmetric, and it prevails in the right tail of $P(q)$. As expected, the contributions of the ipo-friction are negligible on the statistics of q .

We have observed a signature of the presence of strong dissipative events also in the statistical convergence of the moments of q , which displays abrupt changes of the averages during the evolution of the system. A visual inspection of the vorticity field at the time these events occurs, reveals the presence of extremely intense and tiny filaments of vorticity (see Figure 4). These vorticity filaments, which are generated by the chaotic stretching of the direct enstrophy cascade, causes localized events of strong viscous dissipation, which are clearly visible in the corresponding field q_ν [19].

In summary, the results of this set of simulations reveal a significant breaking of the time-asymmetry in the

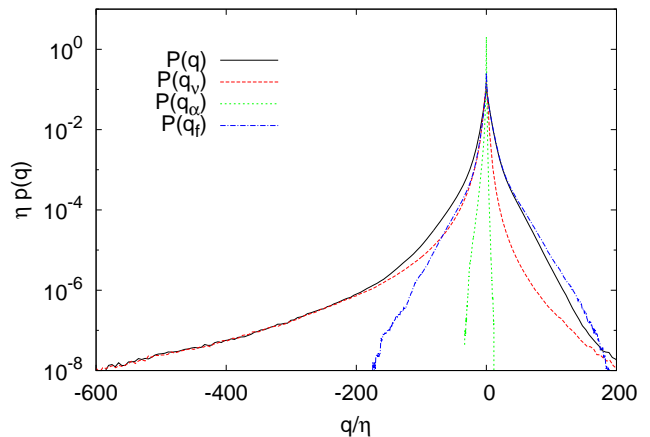


FIG. 3. (Color online). PDF of the metenstrophy q for the case $Re = 1.5 \cdot 10^4$ (back solid line), and of the different contributions: viscosity q_ν (red, dashes line), ipo-friction q_α (green, dotted line), forcing q_f (blue, dash-dotted line).

statistics of the metenstrophy. The irreversibility increases with Reynolds, and it is intrinsically related to the chaotic-stretching nature of the direct enstrophy cascade, which produces tiny and intense filaments of vorticity localized both in space and time.

B. Dependence on the forcing correlation time

Considering that the intense dissipative events must be balanced on average by the forcing, it is natural to suppose that the statistics of the metenstrophy cannot be universal with respect to the forcing itself. We addressed this issue with a second set of simulations (Set B), in which we keep fixed the viscous dissipation and we have changed the time-correlation τ_f of the external forcing. For this purpose, we forced all the wavenumbers in the shell $k \in [k_{f1}, k_{f2}]$ with independent stochastic Ornstein-Uhlenbeck processes $df_{t,\mathbf{k}} = -(1/\tau_f)f_{t,\mathbf{k}}dt + \sqrt{2F}dW_{t,\mathbf{k}}$, where $W_{t,\mathbf{k}}$ are independent Wiener processes. The amplitude F of the forcing has been tuned to obtain (a posteriori) similar enstrophy fluxes in the simulations with different τ_f . We define the mean square forcing wavenumber as $k_F^2 = \langle |\mathbf{k}|^2 \rangle_{k \in [k_{f1}, k_{f2}]}$ and the forcing scale as $\ell_f = 2\pi/k_f$. The parameters of this sec-

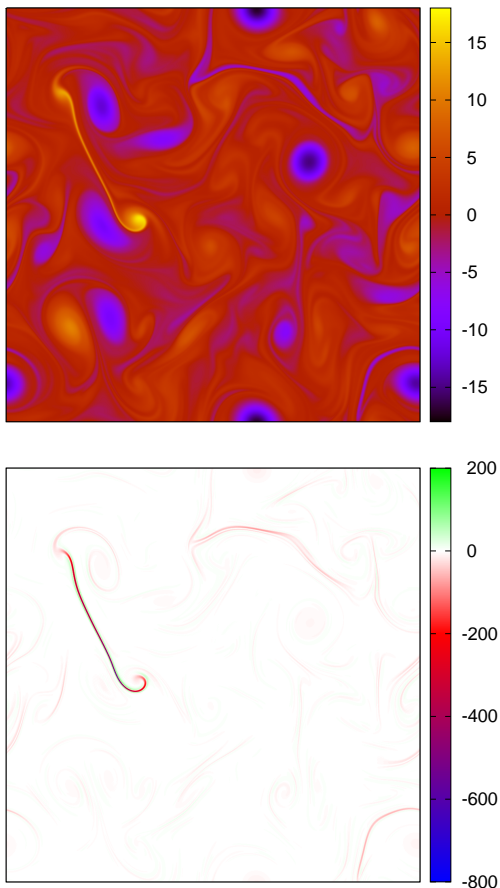


FIG. 4. (Color online). Snapshots of the vorticity field ω (upper plot) and viscous enstrophy dissipation rate q_ν (lower plot) at the same time for the simulation at $Re = 3.7 \cdot 10^3$.

ond set of simulations are reported in Table III B. Also in this case, the statistics is computed over 2000 independent vorticity fields, sampled every $1.2\tau_\omega$.

The PDFs of the metenstrophy computed in simulations with different forcing are shown in Figure 5. In the simulations with a forcing with the long correlation time τ_f we observe PDFs characterized by a strong asymmetry, due to a pronounced left tail, similar to what observe for the stationary forcing of the Set A. However, we find that the asymmetry reduces as we reduce the correlation time of the forcing.

The simmetrization of the PDF is accompanied by a broadening of its tails. This is well captured by the dependence of the second and third moment on τ_f shown in Figure 6. As the correlation time is reduced, we observe an increase of the second moment, which corresponds to the broadening of the PDF's tails, and a reduction of the third moment of the distributions, which indicates the reduction of the asymmetry.

The combined growth of $\langle q^2 \rangle$ and the decrease of $\langle q^3 \rangle$ results in a reduction of the skewness $S = \langle q^3 \rangle / \langle q^2 \rangle^{3/2}$ at reducing the correlation time of the forcing (see Figure 6).

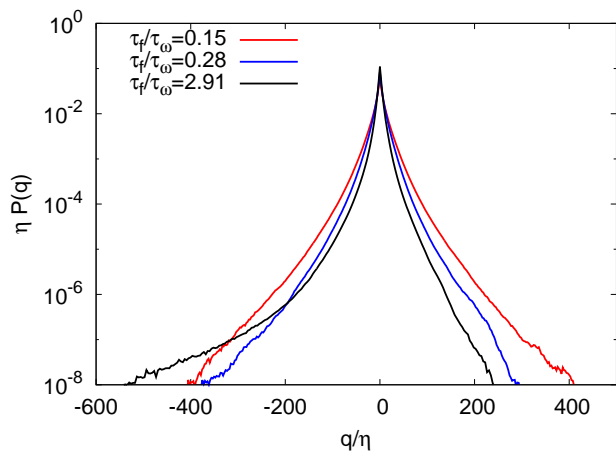


FIG. 5. (Color online). PDFs of metenstrophy q for different correlation times τ_f

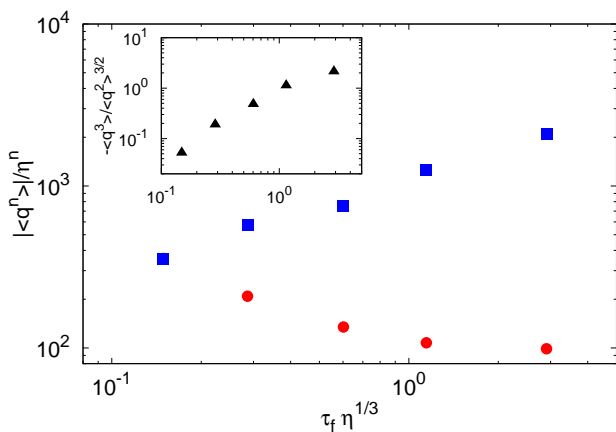


FIG. 6. (Color online). Second (red circles) and third (blue square) moments of the PDFs of metenstrophy q as a function of τ_f . Inset: Skewness of metenstrophy as a function of τ_f .

The analysis of the different contribution to the metenstrophy, (the forcing q_f , the viscous dissipation q_ν and the ipo-friction q_α) reveals that the fluctuations of the forcing are the main responsible for the broadening of the tails observed in the case of short-correlated forcing (see Figure 7). The PDF of the viscous dissipation q_ν displays a clear asymmetry, but its contribution to $P(q)$ is much weaker than that of the forcing.

Our findings can be explained easily. Reducing the time-correlations of the forcing causes also a reduction of the correlation between the force field and the vorticity field. The mean, positive enstrophy input is therefore the result of cancellations between larger and larger positive and negative fluctuations of the input, which have no reason to be asymmetric. The broad, symmetric tails of $P(q_f)$ which develops in the limit $\tau_f \rightarrow 0$ overwhelm the asymmetric contributions of $P(q_\nu)$, originated by the generation of the tiny vorticity filaments.

Re	$\tau_f \eta^{1/3}$	τ_f	F	$-\langle q_\nu \rangle$	$-\langle q_\alpha \rangle$	$\langle q_f \rangle$	E	Z
$1.60 \cdot 10^4$	0.15	0.25	$2.5 \cdot 10^{-1}$	$2.08 \cdot 10^{-1}$	$3.8 \cdot 10^{-2}$	$2.50 \cdot 10^{-1}$	$1.60 \cdot 10^{-1}$	3.52
$1.55 \cdot 10^4$	0.29	0.50	$5.8 \cdot 10^{-2}$	$1.89 \cdot 10^{-1}$	$3.5 \cdot 10^{-2}$	$2.25 \cdot 10^{-1}$	$1.55 \cdot 10^{-1}$	3.45
$1.63 \cdot 10^4$	0.60	1.00	$2.0 \cdot 10^{-2}$	$2.18 \cdot 10^{-1}$	$4.1 \cdot 10^{-2}$	$2.60 \cdot 10^{-1}$	$1.80 \cdot 10^{-1}$	4.05
$1.55 \cdot 10^4$	1.15	2.00	$5.7 \cdot 10^{-3}$	$1.87 \cdot 10^{-1}$	$3.7 \cdot 10^{-2}$	$2.25 \cdot 10^{-1}$	$1.68 \cdot 10^{-1}$	3.90
$1.57 \cdot 10^4$	2.91	5.00	$1.8 \cdot 10^{-3}$	$1.96 \cdot 10^{-1}$	$4.0 \cdot 10^{-2}$	$2.37 \cdot 10^{-1}$	$1.92 \cdot 10^{-1}$	3.53

TABLE II. Parameters of the simulations with Ornstein-Uhlenbeck forcing (Set B). The wavenumber forcing shell is $5 \leq k \leq 6$. The viscosity is $\nu = 5 \cdot 10^{-5}$ and the ipo-friction coefficient is $\alpha = 1$.

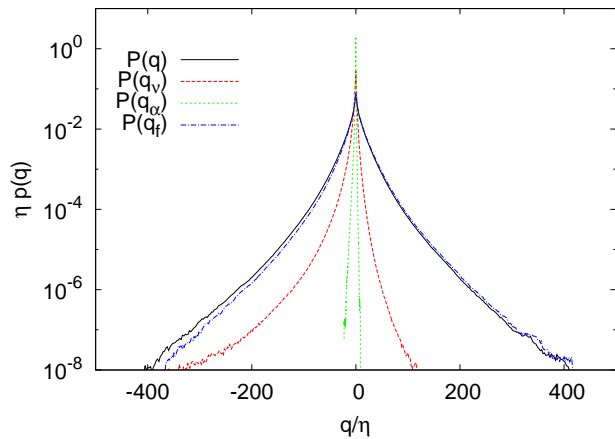


FIG. 7. (Color online). PDF of the metenstrophy q for the case $\tau_f \eta^{1/3} = 0.15$ (back solid line), and of the different contributions: viscosity q_ν (red, dashes line), ipofriction q_α (green, dotted line), forcing q_f (blue, dash-dotted line).

IV. CONCLUSIONS

In this work we have investigated the statistics of the metenstrophy q , that is the time derivative of the enstrophy along a Lagrangian trajectory, in a two-dimensional turbulent flows in the regime of the direct enstrophy cas-

cade sustained by deterministic and stochastic forcing.

The main result of our work is that the statistics of q is characterized by a strong violation of the time-symmetry. The irreversibility increases with the Reynolds number, and it is deeply related to the mechanism of the direct enstrophy cascade, which generates tiny filaments of vorticity by means of chaotic stretching. At the viscous scales, these filaments causes intense events of enstrophy dissipation, therefore giving strong contributions to the left tail of the PDF of q .

Being the results of balance between forcing and dissipation, the statistics of the metenstrophy is also dependent on the forcing mechanisms. In particular we have shown that the irreversibility is reduced in the case of stochastic forcing with short correlation time, whose broad and symmetric fluctuations overwhelms the asymmetric contributions of the viscous dissipation.

The mechanism which causes the symmetry breaking is essentially the chaotic stretching of the flow. This suggests that our results can be extended also to other systems, in particular to the statistics of a scalar field transported a turbulent of a chaotic flow.

More in general, the study of single point irreversibility in different turbulent models will allow to build a general picture of possible universal features of how time symmetry breaking in far from equilibrium systems.

-
- [1] U. Frisch, *Turbulence: The Legacy of AN Kolmogorov* (Cambridge University Press, Cambridge, 1995).
 - [2] G. Falkovich and A. Frishman, Phys. Rev. Lett. **110**, 214502 (2013).
 - [3] H. Xu, A. Pumir, G. Falkovich, E. Bodenschatz, M. Shats, H. Xia, N. Francois, and G. Boffetta, Proc. Natl. Acad. Sciences **111**, 7558 (2014).
 - [4] A. Pumir, H. Xu, E. Bodenschatz, and R. Grauer, Phys. Rev. Lett. **116**, 124502 (2016).
 - [5] G. Boffetta and R. Ecke, Annu. Rev. Fluid Mech. **44**, 427 (2012).
 - [6] T. Grafke, A. Frishman, and G. Falkovich, Phys. Rev. E **91**, 043022 (2015).
 - [7] A. Pumir, H. Xu, G. Boffetta, G. Falkovich, and E. Bodenschatz, Phys. Rev. X **4**, 041006 (2014).
 - [8] R. Kraichnan, Phys. Fluids **10**, 1417 (1967).
 - [9] G. Boffetta and S. Musacchio, Phys. Rev. E **82**, 016307 (2010).
 - [10] M. Maltrud and G. Vallis, J. Fluid Mech. **228**, 321 (1991).
 - [11] V. Borue, Phys. Rev. Lett. **71**, 3967 (1993).
 - [12] T. Gotoh, Phys. Rev. E **57**, 2984 (1998).
 - [13] A. Belmonte, W. Goldburg, H. Kellay, M. Rutgers, B. Martin, and X. Wu, Phys. Fluids **11**, 1196 (1999).
 - [14] E. Lindborg and K. Alvelius, Phys. Fluids **12**, 945 (2000).
 - [15] C. Pasquero and G. Falkovich, Phys. Rev. E **65**, 056305 (2002).
 - [16] S. Chen, R. Ecke, G. Eyink, X. Wang, and Z. Xiao, Phys. Rev. Lett. **91**, 214501 (2003).
 - [17] M. Rivera, W. Daniel, S. Chen, and R. Ecke, Phys. Rev. Lett. **90**, 104502 (2003).
 - [18] G. Boffetta, A. Celani, S. Musacchio, and M. Vergassola,

Phys. Rev. E **66**, 026304 (2002).

[19] A. Bracco and J. McWilliams, J. Fluid Mech. **646** (2010).